Supplementary Information for:

Metallic-nanowire-loaded silicon-on-insulator structures: a route to low-loss plasmon waveguiding on the nanoscale

Yusheng Bian[1] and Qihuang Gong[1,2*]

[1]State Key Laboratory for Mesoscopic Physics, Department of Physics, Peking University, Beijing 100871, China

[2]Collaborative Innovation Center of Quantum Matter, Beijing, China

**Corresponding Author. Email: qhgong@pku.edu.cn*

S1. FoMs of MNLSOIW and other typical plasmonic waveguides

In Supplementary Table 1, we show the calculated FoMs (defined as the ratio of the propagation length to the effective mode size [1]) of MNLSOIW and other typical plasmonic structures, including MNW, HPW, dielectric-loaded surface plasmon polariton waveguide (DLSPPW) [2], channel plasmon polariton waveguide (CPPW) [3], plasmonic slot waveguide (PSW) [4], long-range surface plasmon polariton waveguide (LRSPPW) [5] and long-range dielectric-loaded surface plasmon polariton waveguide (LRDLSPPW) [6, 7]. For MNLSOIW, MNW and HPW structures, the best FoMs that can be achieved within the range of the considered dimensions (Fig. 5 of the paper) have been listed. For CPPW, the groove depth is 1.5 μm and the groove angle is chosen at 16°, whereas the top and bottom corners of the groove are rounded with 100 nm and 10 nm curvatures, respectively [8]. The metallic groove is assumed to be placed in an air cladding. The size of the slot region of PSW is set at 50 nm by

50 nm, and the metal films are assumed to be embedded in a SiO_2 background [9]. The DLSPPW consists of a PMMA ridge (600nm by 600nm) on top of a metallic substrate with an air cladding [2], whereas the LRSPPW comprises a thin silver film (2 μm by 30 nm) embedded in silica [5]. The dimensions and materials of LRDLSPPW are the same as in [10], except for the material of the metallic layer. As clearly illustrated from Suppl. Table 1, our proposed MNLSOIW features much larger FoM than other popular subwavelength plasmonic waveguiding structures, such as MNW, HPW, DLSPPW, CPPW and PSW. On the other hand, although the FoMs of LRSPPW and LRDLSPPW exceed that of the MNLSOIW, these waveguides could not offer nanoscale field confinement, thereby rendering themselves less suitable for compact photonic integrations.

Waveguide	MNLSOIW	MNW	HPW	DLSPPW
FoM	1710	333	458	338
Waveguide	CPPW	PSW	LRSPPW	LRDLSPPW
FoM	219	435	7601	18234

Supplementary Table 1: Comparisons of FoMs of typical plasmonic waveguides. To allow for fair comparisons between different structures, the metallic layers of all these configurations are assumed to be made of silver, while exactly the same method for the calculation of the mode size has been adopted. The operating wavelength is fixed at 1550 nm. Note that the FoMs of PSW and LRSPPW are larger than those listed in [11], which are due to the different refractive indices of the silica layer adopted (1.444 employed here and 1.5 used in [11]).

S2. Bending properties of MNLSOIWs

In addition to the crosstalk between adjacent waveguides, bending property is another important factor that could determine the waveguide's performance for compact photonic integrations [10, 12]. Here we evaluate the bending characteristics of MNLSOIWs by performing full-wave 3D FEM simulations. In Suppl. Fig.1, we show

the calculated light transmission through a 90° MNLSOIW bend as a function of the bending radius. Note that both the radiation loss and the propagation loss are considered during the simulations. It is shown that the overall transmission of light that propagates through a 90° bend based on the MNLSOIW can be larger than 70% when the bend radius falls within the range of 0.2 μm - 1μm, which is quite beneficial for building ultra-compact photonic devices. With the increase of the bend radius, the transmission increases first before it decreases, resulting in an optimal bending radius that corresponds to the highest transmission. For the considered MNLSOIW bend in our case study, the optimal bending radius is around 0.4 μm, where the transmission of light exceeds 80%. The above results clearly indicate the good capability of the waveguide for routing light through sharp bends.

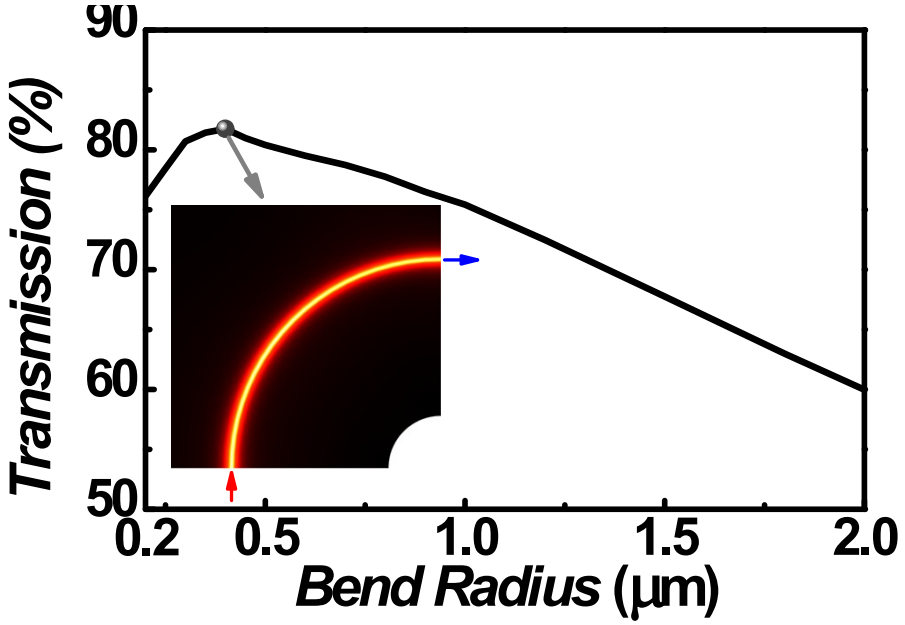

Supplementary Figure 1: Transmission of light through a 90° bend as a function of the bend radius. The structural parameters for the MNLSOW involved are r = 20 nm, t = 40 nm, g = 2 nm. The inset gives the transmitted electric field distribution for a waveguide bend with a 0.4 μm bending radius. Red and blue arrows indicate the directions of the incoming light and outcoming light, respectively.

While considering gain-assisted light guiding of MNLSOWs, it is here worth

mentioning that for the optical pump method, the presence of the metallic nanowire may partially block the laser beam if the pump light is incident from the top, which might increase the difficulty of loss compensation. To overcome this challenge, the pump light can be introduced through back-side illumination, i.e., incident from the substrate, similar to the previously studied active hybrid waveguides [13, 14]. On the other hand, near-field coupling techniques, such as those employing (tapered) optical fibers [15, 16], might also be employed for optical pumping. We also note that, for our studied MNLSOIWs, the pump may also be provided in electric ways [17], although such methods could be much more complex. These issues deserve further discussions in our later studies.

S3. Alternative configurations

In addition to the metallic-nanowire-loaded silicon-on-insulator structures discussed in the paper, the waveguide concept that merges nanowire plasmon transport with dielectric waveguiding can also be extended to other metal-dielectric configurations. Here, we show two typical types of modified MNLSOIWs, which are obtained by combining the current design with those of those of hybrid metal-insulator-metal (MIM) [18, 19] or insulator-metal-insulator (IMI) [20-22] structures. As schematically illustrated in Suppl. Figs.2(a)-(b), the MIM-type MNLSOIW, which introduces another Ag nanowire on the SOI substrate, offers the potential of strongly localizing the mode field within the slot region between the closely spaced Ag nanowires, while also exhibiting reasonable enhancement inside the gap area between the nanowire and the Si layer. Although this type of waveguide suffers relatively

larger loss as compared to the single-nanowire-based MNLSOIW studied in the paper, its mode area is significantly smaller and the optical confinement is much better. On the other hand, the IMI-type MNLSOIW incorporates another Si layer on top of the Ag nanowire (see Suppl. Figs.2(c)-(d)), which allows further reduction of the modal attenuation of the traditional MNLSOIW due to the unique symmetric hybrid configuration [20], although the corresponding mode size increases slightly. Owing to its ultra-low transmission loss, the IMI-type nanowire waveguide can also be named as long-range MNLSOIWs. Detailed studies relating to these modified MNLSOIWs will be reported in our forthcoming articles.

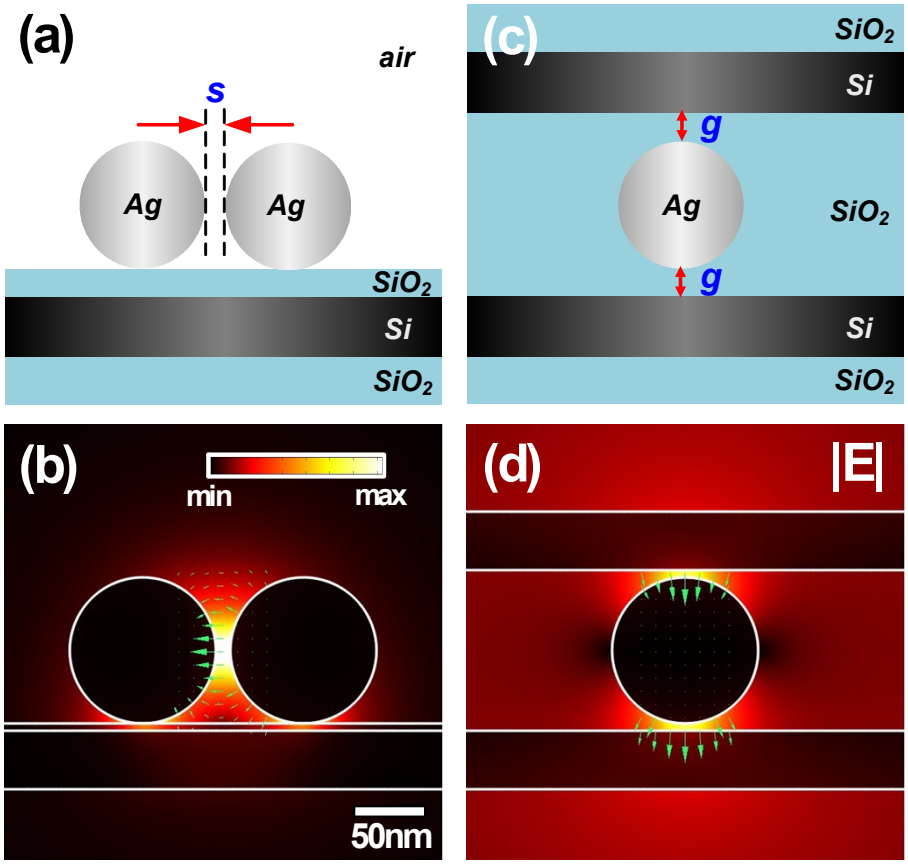

Supplementary Figure 2: (a)-(b) 2D schematic of MIM-type MNLSOIW and electric field distribution of the highly confined quasi-TE plasmonic mode (r = 50 nm, t = 40 nm, g = 5 nm, s = 10 nm); (c)-(d) Schematic illustration of IMI-type MNLSOIW and field profile of its guided symmetric low-loss mode (r = 50 nm, t = 40 nm, g = 5 nm).

References

1. R. Buckley, and P. Berini, "Figures of merit for 2D surface plasmon waveguides and application to metal stripes," Opt. Express **15**(19), 12174-12182 (2007).
2. T. Holmgaard, and S. I. Bozhevolnyi, "Theoretical analysis of dielectric-loaded surface plasmon-polariton waveguides," Phys. Rev. B **75**(24), 245405 (2007).
3. S. I. Bozhevolnyi, V. S. Volkov, E. Devaux, J. Y. Laluet, and T. W. Ebbesen, "Channel plasmon subwavelength waveguide components including interferometers and ring resonators," Nature **440**(7083), 508-511 (2006).
4. L. Liu, Z. Han, and S. He, "Novel surface plasmon waveguide for high integration," Opt. Express **13**(17), 6645-6650 (2005).
5. P. Berini, "Long-range surface plasmon polaritons," Adv. Opt. Photonics **1**(3), 484-588 (2009).
6. V. S. Volkov, Z. Han, M. G. Nielsen, K. Leosson, H. Keshmiri, J. Gosciniak, O. Albrektsen, and S. I. Bozhevolnyi, "Long-range dielectric-loaded surface plasmon polariton waveguides operating at telecommunication wavelengths," Opt. Lett. **36**(21), 4278-4280 (2011).
7. J. Gosciniak, T. Holmgaard, and S. I. Bozhevolnyi, "Theoretical Analysis of Long-Range Dielectric-Loaded Surface Plasmon Polariton Waveguides," J. Lightwave Technol. **29**(10), 1473-1481 (2011).
8. E. Moreno, S. G. Rodrigo, S. I. Bozhevolnyi, L. Martin-Moreno, and F. J. Garcia-Vidal, "Guiding and focusing of electromagnetic fields with wedge plasmon polaritons," Phys. Rev. Lett. **100**(2), 023901 (2008).
9. G. Veronis, and S. H. Fan, "Modes of subwavelength plasmonic slot waveguides," J. Lightwave Technol. **25**2511-2521 (2007).
10. Z. H. Han, and S. I. Bozhevolnyi, "Radiation guiding with surface plasmon polaritons," Rep. Prog. Phys. **76**(1), 016402 (2013).
11. Y. S. Bian, Z. Zheng, X. Zhao, L. Liu, Y. L. Su, J. Xiao, J. S. Liu, J. S. Zhu, and T. Zhou, "Dielectrics Covered Metal Nanowires and Nanotubes for Low-Loss Guiding of Subwavelength Plasmonic Modes," J. Lightwave Technol. **31**(12), 1973-1979 (2013).
12. W. Wang, Q. Yang, F. Fan, H. Xu, and Z. L. Wang, "Light Propagation in Curved Silver Nanowire Plasmonic Waveguides," Nano Lett. **11**(4), 1603-1608 (2011).
13. J. Zhang, L. Cai, W. Bai, Y. Xu, and G. Song, "Hybrid plasmonic waveguide with gain medium for lossless propagation with nanoscale confinement," Opt. Lett. **36**(12), 2312-2314 (2011).
14. D. Dai, Y. Shi, S. He, L. Wosinski, and L. Thylen, "Gain enhancement in a hybrid plasmonic nano-waveguide with a low-index or high-index gain medium," Opt. Express **19**(14), 12925-12936 (2011).
15. W. Wei, Y. Liu, X. Zhang, Z. Wang, and X. Ren, "Evanescent-wave pumped room-temperature single-mode GaAs/AlGaAs core-shell nanowire lasers," Appl. Phys. Lett. **104**(22), 223103 (2014).
16. X. Q. Wu, Y. Xiao, C. Meng, X. N. Zhang, S. L. Yu, Y. P. Wang, C. X. Yang, X. Guo, C. Z. Ning, and L. M. Tong, "Hybrid Photon-Plasmon Nanowire Lasers," Nano Lett. **13**(11), 5654-5659 (2013).
17. M. T. Hill, Y.-S. Oei, B. Smalbrugge, Y. Zhu, T. De Vries, P. J. Van Veldhoven, F. W. M. Van Otten, T. J. Eijkemans, J. P. Turkiewicz, H. De Waardt, E. J. Geluk, S.-H. Kwon, Y.-H. Lee, R. Notzel, and M. K. Smit, "Lasing in metallic- Coated nanocavities," Nature Photonics **1**(10), 589-594 (2007).
18. Y. S. Bian, and Q. H. Gong, "Optical performance of one-dimensional hybrid metal-insulator-metal structures at telecom wavelength," Opt. Commun. **308**30-35 (2013).

19. L. Lafone, T. P. H. Sidiropoulos, and R. F. Oulton, "Silicon-based metal-loaded plasmonic waveguides for low-loss nanofocusing," Opt. Lett. **39**(15), 4356-4359 (2014).
20. Y. S. Bian, Z. Zheng, X. Zhao, J. S. Zhu, and T. Zhou, "Symmetric hybrid surface plasmon polariton waveguides for 3D photonic integration," Opt. Express **17**(23), 21320-21325 (2009).
21. Y. S. Bian, and Q. H. Gong, "Low-loss light transport at the subwavelength scale in silicon nano-slot based symmetric hybrid plasmonic waveguiding schemes," Opt. Express **21**(20), 23907-23920 (2013).
22. Y. S. Bian, and Q. H. Gong, "Long-range hybrid ridge and trench plasmonic waveguides," Appl. Phys. Lett. **104**(25), 251115 (2014).